Role of Vapor−Phase Mass Transport During the Spreading of a Long−Chain Alkane Drop

ARTICLE *in* LANGMUIR · AUGUST 2009

Impact Factor: 4.46 · DOI: 10.1021/la9016917 · Source: PubMed

2 AUTHORS, INCLUDING:

Lingbo Lu
University of Kentucky
9 PUBLICATIONS **32** CITATIONS

Langmuir
Letter
pubs.acs.org/Langmuir

Role of Vapor-Phase Mass Transport During the Spreading of a Long-Chain Alkane Drop†

Lingbo Lu and Yuguang Cai*

Department of Chemistry, University of Kentucky, Rose Street, Lexington, Kentucky 40506

Received May 12, 2009. Revised Manuscript Received June 15, 2009

The spreading of liquid alkanes over solid surfaces has important applications in painting, coatings, lubrication, and petroleum tertiary recovery. The role of the vapor-phase mass transport accompanying liquid spreading has not been well studied because it is difficult to separate the contributions from the liquid spreading and the vapor-phase transport that occurred at the same time. We used the engineered surface patterns to study the vapor-phase mass transport during liquid spreading. First, we fabricated several hydrophilic, carboxylic acid-terminated patterns (OTSpd) on a hydrophobic, methyl-terminated octadecyltrichlorosilane (OTS) surface. These OTSpd patterns did not connect to each other. Next, we let an alkane drop spread within one OTSpd pattern. The liquid alkane could not spread to other OTSpd patterns because OTS separated them; however, the alkane molecules in the vapor phase could migrate and adsorb on other OTSpd patterns. Therefore, the contributions from the liquid spreading and the vapor-phase transport were separated and could be investigated independently. We found that during the spreading of the liquid alkane, mass transport through the vapor phase cannot be ignored. Alkane molecules adsorbed on the OTSpd surface with their backbones parallel to the surface in the first few layers. Additional alkane molecules adsorbed on these parallel layers to form the seaweed-shaped layers in which the alkane molecules stood up. Our study showed that the parallel layers formed from the vapor-phase mass transport before the liquid alkane spread. Therefore, the liquid alkane does not spread over the more strongly binding OTSpd surface. It actually spreads over the parallel alkane layer, which formed from its own vapor.

Introduction

Liquid spreading over a solid surface has important applications in painting, coatings, lubrication, and irrigation.[1] Liquid spreading has been extensively studied.[1−14] During spreading, molecular transport is not limited within the liquid phase but can extend to the gas phase also. For instance, interfacial gas-phase transport caused the growth of the mesa-shape particle in the dotriacontane (C32) film.[11] Despite a few pioneering attempts,[3,11,15,16] the role of vapor-phase mass transport during spreading is not well understood. When a drop spreads over a solid surface, molecules in the liquid's vapor also adsorb onto the solid surface. These adsorbates change the surface properties, which in turn affect both the kinetic and thermodynamic parameters of the spreading. Most experiments and theory ignore the effect of vapor-phase mass transport because of the technical difficulties of separating the contributions from the liquid transport and gas-phase transport during spreading. In an alternative approach, the spreading of a droplet on top of a preadsorbed film has been reported, which shows the importance of the preadsorbed film on the dynamics of the liquid spreading.[17,18]

The spreading of alkanes has attracted special attention because liquid alkanes have been extensively used in lubrication, painting, and printing. After spreading, when the sample was cooled to below the alkanes' melting points, long-chain *n*-alkanes adopt the bilayer structure on the more strongly binding surface (such as SiO_2).[8,19] In the bilayer structure, the alkane molecules adsorb on the surface with their chains parallel to the surface, forming the parallel layer. On top of one or several parallel layers, additional alkane molecules stand up, forming a seaweed-shaped layer in which alkane molecules stand vertically or tilt at certain angles. The parallel layer formed before the standing-up layer because the standing-up seaweed-shaped layer is on top of the parallel layer(s). However, it is not clear whether the parallel layer was formed from the liquid spreading itself or from the vapor-phase transport accompanying the liquid spreading.

In this letter, we used engineered surface patterns to study the vapor-phase transport during the spreading of liquid alkanes. We

† Part of the "Langmuir 25th Year: Self-assembled monolayers: synthesis, characterization, and applications" special issue.

*Corresponding author. E-mail: ycai3@uky.edu.

(1) de Gennes, P. G. *Rev. Mod. Phys*. **1985**, *57*, 827.
(2) Sukhishvili, S. A.; Chen, Y.; Müller, J. D.; Gratton, E.; Schweizer, K. S.; Granick, S. *Nature* **2000**, *406*, 146.
(3) Gallyamov, M. O.; Tartsch, B.; Mela, P.; Potemkin, I. I.; Sheiko, S. S.; Borner, H.; Matyjaszewski, K.; Khokhlov, A. R.; Moller, M. *J. Polymer Sci., Part B* **2007**, *45*, 2368.
(4) Xu, H.; Shirvanyants, D.; Beers, K.; Matyjaszewski, K.; Rubinstein, M.; Sheiko, S. S. *Phys. Rev. Lett*. **2004**, *93*, 206103.
(5) Xu, L.; Lio, A.; Hu, J.; Ogletree, D. F.; Salmeron, M. *J. Phys. Chem. B* **1998**, *102*, 540.
(6) Hu, J.; Carpick, R. W.; Salmeron, M.; Xiao, X. D. *J. Vac. Sci .Technol., B* **1996**, *14*, 1341.
(7) Lazar, P.; Schollmeyer, H.; Riegler, H. *Phys. Rev. Lett*. **2005**, *94*, 116101.
(8) Mo, H.; Taub, H.; Volkmann, U. G.; Pino, M.; Ehrlich, S. N.; Hansen, F. Y.; Lu, E.; Miceli, P. *Chem. Phys. Lett*. **2003**, *377*, 99.
(9) Trogisch, S.; Simpson, M. J.; Taub, H.; Volkmann, U. G.; Pino, M.; Hansen, F. Y. *J. Chem. Phys*. **2005**, *123*, 154703.
(10) Wu, Z.; Ehrlich, S. N.; Matthies, B.; Herwig, K. W.; Dai, P.; Volkmann, U. G.; Hansen, F. Y.; Taub, H. *Chem. Phys. Lett*. **2001**, *348*, 168.
(11) Bai, M.; Knorr, K.; Simpson, M. J.; Trogisch, S.; Taub, H.; Ehrlich, S. N.; Mo, H.; Volkmann, U. G.; Hansen, F. Y. *Europhys. Lett*. **2007**, *79*, 26003.
(12) Riegler, H.; Kohler, R. *Nat. Phys*. **2007**, *3*, 890.
(13) Honciuc, A.; Howard, A. L.; Schwartz, D. K. *J. Phys. Chem. C* **2009**, *113*, 2078.
(14) Honciuc, A.; Harant, A. W.; Schwartz, D. K. *Langmuir* **2008**, *24*, 6562.
(15) Carles, P.; Cazabat, A. M. *Prog. Colloid Polym. Sci*. **1990**, *82*, 76.
(16) Aveyard, R.; Beake, B. D.; Clint, J. H. *Phys. Chem. Chem. Phys*. **1999**, *1*, 2513.
(17) Ajaev, V. S. *J. Fluid Mech*. **2005**, *528*, 279.
(18) Glasner, K. B. *Phys. Fluids* **2003**, *15*, 1837.
(19) Basu, S.; Satija, S. K. *Langmuir* **2007**, *23*, 8331.

fabricated a series of discrete, carboxylic acid-terminated patterns (OTSpd) on the nonspreadable, methyl-terminated surface. When an alkane drop spread within one OTSpd pattern, molecules in liquid were limited within this OTSpd pattern, and molecules in the vapor adsorbed on the surfaces of all OTSpd patterns. After spreading, by comparing the OTSpd surface where a liquid alkane had spread and the OTSpd surface where only vapor-phase adsorption had occurred, we separated the contributions from the liquid- and vapor-phase mass transport. We found that during liquid alkane spreading the vapor-phase mass transport played a significant role, which cannot be ignored. Alkane molecules in the vapor phase adsorbed on the OTSpd surface *before* the liquid−solid contact line arrived. The parallel alkane layer was formed from the vapor-phase transport. Therefore, our data strongly suggest that when an alkane drop starts to spread over a more strongly binding surface, the liquid does not really spread directly on the more strongly binding surface. Instead, it actually spreads over the parallel alkane layer that formed from its own vapor.

Methods and Instruments

We used scanning probe deep oxidation lithography to fabricate OTSpd chemical patterns on an octadecyltrichlorosilane film (OTS film) surface.[20,21] The precursor molecule, octadecyltrichlorosilane, hydrolyzed to silanol. Then the silanol molecules cross-linked and were anchored on the hydroxyl-terminated SiO_2 surface to form the methyl-terminated OTS film. The OTS film is hydrophobic and ultraflat, with a root mean square (rms) roughness of < 5 Å. In a humid environment, we applied a $+10$ V bias to the OTS-coated wafer. The OTS film under a conducting atomic force microscope (AFM) tip (Pt−Ti-coated, CSC-17, MikroMacsh) was oxidized to carboxylic acid-terminated, partially degraded silane (OTSpd). The detailed procedures for OTS film preparation and OTSpd pattern fabrication have been documented elsewhere.[21] The OTSpd has a more strongly binding surface and is 10.2 ± 0.7 Å lower than the OTS background.[21] The liquid alkane can spread over the OTSpd surface. In contrast, OTS is a methyl-terminated, less strongly binding surface over which the liquid alkane cannot spread.

Scheme 1 illustrates our experimental procedure. First, we fabricated a small OTSpd dot on the OTS surface (Scheme 1a, blue dot). Next, we dip-coated the sample with molten hexatriacontane ($C_{36}H_{74}$). Because OTSpd has a more strongly binding surface and OTS has a less strongly binding surface, hexatriacontane stayed only on the OTSpd surface after dip-coating (Scheme 1b). When cooled, the alkane on OTSpd froze. We then fabricated a few "satellite" OTSpd disks, which were 2−20 μm away from the alkane drop (Scheme 1c). Subsequently, we used the conducting AFM probe to fabricate another "large" main OTSpd disk, which enclosed the alkane drop and did not connect to the satellite OTSpd disks (Scheme 1d). In a control test, we followed the above procedure and fabricated a sample that was the same as for Scheme 1d. Then we wiped the sample with chloroform to remove the alkane completely. The subsequent AFM characterization indicated that the OTSpd dot fabricated in Scheme 1a and the OTSpd disk fabricated in Scheme 1c, fused together.[21] There was no OTS between the OTSpd dot fabricated in Scheme 1a and the OTSpd disk fabricated in Scheme 1c. The AFM topography image and the phase image showed that the fused disk was topographically and chemically homogeneous. The control experiment demonstrates that the two-step patterning method (as shown in Scheme 1) can be used to fabricate a spreadable homogeneous surface surrounding the solidified alkane. When melted, the liquid alkane could spread over the main disk freely. Then, after pattern fabrication, we raised the sample temperature to 90 °C in air to melt the frozen alkane and to trigger

Scheme 1. OTSpd Dot and Disk Fabrication[a]

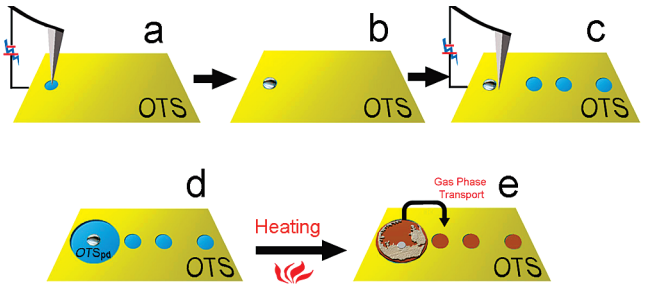

[a] (a) The OTSpd disk pattern was fabricated by local probe deep oxidation. (b) *n*-Hexatriacontane was dip-coated onto the OTSpd pattern. After the OTSpd pattern was briefly dipped into liquid *n*-hexatriacontane, the alkane drop adsorbed and solidified on the OTSpd pattern. (c) A few satellite OTSpd disks were fabricated on the OTS surface, which were 2−20 μm away from the alkane drop. Then we moved the conducting AFM tip into the vicinity of the alkane drop and imparted a voltage pulse to the tip. Thus, a new OTSpd disk (the main disk (blue)) was fabricated surrounding the coated *n*-hexatriacontane by local probe deep oxidation. The main disk did not connect to those satellite disks. (d) At room temperature, coated *n*-hexatriacontane was a solid. There was no spreading. (e) When heated, the alkane drop melted. The liquid alkane spread over the OTSpd main disk, whereas the alkane molecules were deposited on the satellite OTSpd disks through vapor-phase transport. Upon cooling, the alkane liquid froze. Then the alkane structures could be characterized by AFM.

alkane spreading. After 30 s, we cooled the sample to room temperature rapidly. The rapid cooling stopped the spreading and suppressed the surface freezing of the liquid alkane.[22] The liquid alkane solidified again. Finally, we used AFM to characterize the results of the spreading (Scheme 1e) immediately. The surface characterizations were completed within 1 h.

Surface characterization was performed by using the Agilent PicoPlus 3000 environmental AFM. All AFM images were processed with WSxM.[23]

Results and Discussion

Alkanes Adsorbed on the Satellite OTSpd Disks after Spreading. After alkane spreading, we found that alkane molecules also adsorbed onto the satellite disks, which did not connect to the OTSpd main disk. Figure 1a shows both the main OTSpd disk and the satellite OTSpd disk (in the green box) after alkane spreading. The OTSpd chemical pattern was 10 Å lower than the OTS surface before liquid alkane spreading. After spreading, both the main OTSpd disk and the satellite OTSpd disk appeared to be higher than the OTS background. In the control test, the clean OTSpd patterns were placed in the AFM environmental chamber for 1 h before AFM characterization. The results show that the OTSpd pattern remained 10 Å lower than the OTS pattern, indicating that the environmental contaminants were not the source of the additional material on the OTSpd disk. Because the hydrophobic OTS acted as a barrier between the main disk and the satellite disks, the liquid alkane could not spread from the main disk to the satellite disks. Therefore, the observed additional materials on OTSpd after liquid spreading are the alkane molecules transported from the vapor phase.

Alkanes on the Satellite OTSpd Disk Form Parallel Alkane Layers through Vapor-Phase Transport. Long-chain alkanes form bilayer structures on more strongly binding surfaces.[24] In the main disk, the alkane formed seaweed-shaped

(20) Maoz, R.; Cohen, S. R.; Sagiv, J. *Adv. Mater.* **1999**, *11*, 55.
(21) Cai, Y. G. *Langmuir* **2009**, *25*, 5594.
(22) Wu, X. Z.; Sirota, E. B.; Sinha, S. K.; Ocko, B. M.; Deutsch, M. *Phys. Rev. Lett.* **1993**, *70*, 958.
(23) Horcas, I.; Fernandez, R.; Gomez-Rodriguez, J. M.; Colchero, J.; Gomez-Herrero, J.; Baro, A. M. *Rev. Sci. Instrum.* **2007**, *78*, 013705.
(24) Bai, M.; Trogisch, S.; Magonov, S.; Taub, H. *Ultramicroscopy* **2008**, *108*, 946.

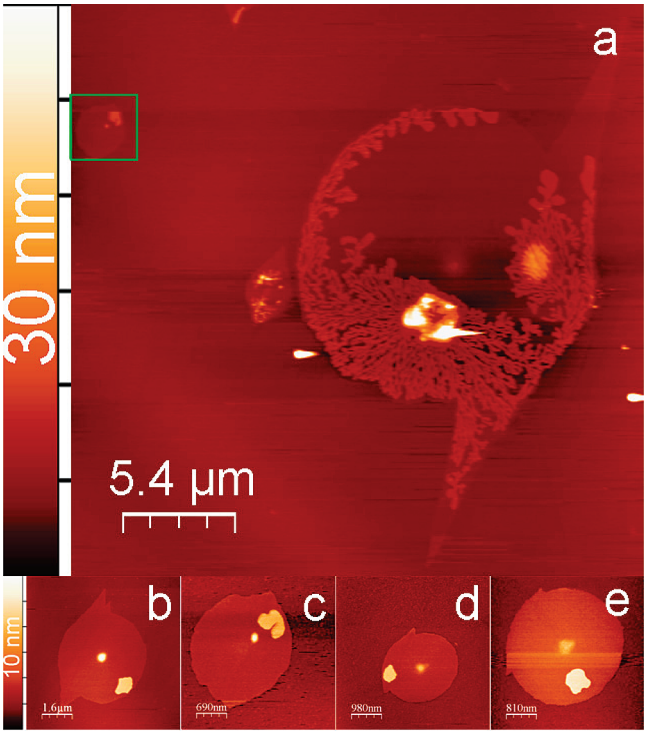

Figure 1. Main OTSpd disk and satellite OTSpd disks after spreading. ac-mode AFM topography images showing (a) the main OTSpd disk and a nearby satellite OTSpd disk (in the green box). (b–e) Satellite OTSpd disks. The same OTSpd disk is located in image c and in the green box of image a. (b, d, e) Satellite OTSpd disks outside the view of image a.

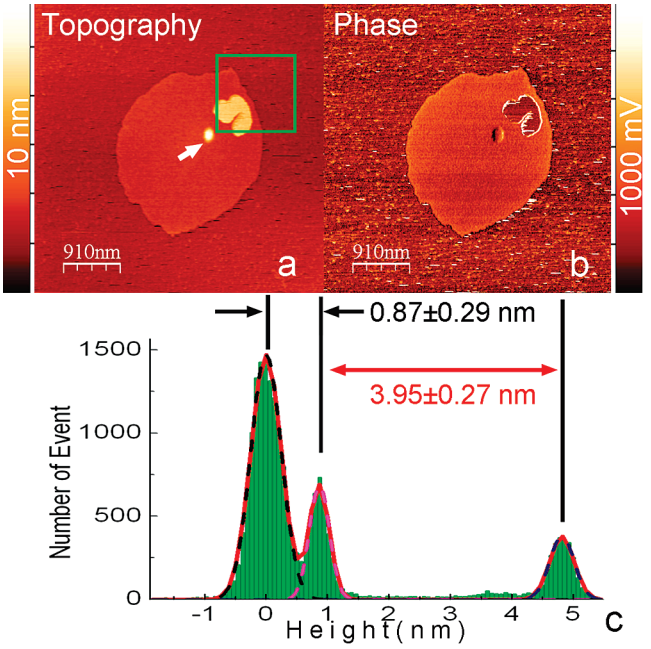

Figure 2. Satellite OTSpd disk after spreading. (a, b) ac-mode topography and phase image, respectively. (c) Height histogram inside the green box in image a. The histogram indicates that the height of the parallel layer is 0.87 ± 0.29 nm above the OTS and that the height of the standing-up alkane layer is 3.95 ± 0.27 nm above the parallel layer.

patterns after the sample was cooled to 25 °C. The seaweed-shaped pattern formed on top of parallel alkane layers, which covered the entire OTSpd surface. Figure 1 shows that the parallel alkane layers are higher than the OTS in the main disk. In the corresponding phase image (not shown), the phase signal of the seaweed-shaped pattern is −1971 ± 195 mV, which is the same as the OTS background because both of them are methyl-terminated. In contrast, the phase signal over the parallel alkane layer is 122 ± 47 mV, which is significantly different from that of the seaweed-shaped alkane layer.

Next, we compared the topography and phase contrast of the main disk with that of satellite disks. Figure 1b–e shows enlarged views of the satellite disks. The satellite OTSpd disk in Figure 1a (inside the green box) is shown in Figure 1c at higher resolution. The satellite disks shown in Figure 1b,d,e are located outside the field of view in Figure 1a. These AFM images of the satellite OTSpd disks are the representative images of more than 30 satellite disks that were characterized in the alkane spreading experiment. All AFM topography images of the satellite disks share similar features. All of the satellite disks are higher than the OTS background after alkane spreading. In the corresponding phase image of Figure 1a (not shown), the value of the phase signal over the satellite disk is 185 ± 78 mV. The phase signal in ac-mode AFM reflects the surface property. Usually, the phase signals over different images are not suitable for comparison because the phase signals are subject to the conditions of the tip status and imaging parameters during scanning. However, in Figure 1a, the main disk and the satellite disk are in the same image and were scanned using the same tip at the same time with the same tip status and imaging parameters. Therefore, in this case, we can compare their surface properties using the phase signals. The value of the phase signal over the parallel alkane layer on the main disk (122 ± 47 mV) is not significantly different from the value of the phase signal over the satellite disk (185 ± 78 mV). The parallel layers on the main disk and the additional material on the OTSpd satellite disk have the same surface property.

Because we know that the additional materials on the satellite OTSpd disks are from vapor-phase transport, we conclude that the satellite disk is also covered with layers of parallel alkane. The alkane molecules on the satellite disk were transported through the vapor phase.

Higher-Resolution AFM Image in Figure 2 Reveals Alkane Structures on the OTSpd Satellite Disk. Both the parallel layer and the seaweed-shaped standing-up layer are present in Figure 2. The height histogram in the green box in Figure 2a is plotted in Figure 2c. The histogram shows that the parallel alkane layer is 0.87 ± 0.29 nm above the OTS and the standing-up alkane layer is 3.95 ± 0.27 nm above the parallel layer. The depth of the OTSpd chemical pattern provides a height reference for calculating the thickness of the parallel layer on OTSpd. We already know that the OTSpd pattern was 1.02 ± 0.07 nm lower than the OTS background before alkane spreading.[21] From the apparent height value obtained from the histogram in Figure 2c and the depth of the OTSpd pattern, we calculated the thickness of the parallel layer to be 1.89 ± 0.30 nm. Using the same histogram analysis, we also obtained the thickness of the parallel layers in Figure 1b,d,e. These values are summarized in Table 1. Assuming that the alkane chain–chain distance is around 0.464 nm,[25] the thickness values listed in Table 1 correspond to four or five parallel alkane layers stacked together. By averaging the calculated thickness values of the single parallel alkane layer listed in Table 1, our data show that one parallel alkane layer is 0.47 ± 0.04 nm, which is consistent with results reported by other groups within the uncertainty range.[25,26] We

(25) Herwig, K. W.; Matthies, B.; Taub, H. *Phys. Rev. Lett.* **1995**, *75*, 3154.
(26) Rabe, J. P.; Buchholz, S. *Phys. Rev. Lett.* **1991**, *66*, 2096.

Table 1. Thickness of Parallel Alkane Layer

OTSpd Disk in Figure 1	Total Thickness (nm)	Number of Parallel Alkane Layers	Calculated Thickness of a Single Parallel Alkane Layer (nm)
b	1.82 ± 0.30	4	0.46 ± 0.08
c	1.89 ± 0.30	4	0.47 ± 0.08
d	2.27 ± 0.48	5	0.45 ± 0.10
e	2.44 ± 0.36	5	0.49 ± 0.07

have characterized the parallel layers on more than 30 satellite OTSpd disks in our spreading experiment. The thickness of the parallel layer varied. The layer thickness values corresponding to one to five layers were all observed. Among all samples we characterized, the four- or five-layer-thick case is the most typical one.

In Figure 2, the thickness (3.95 ± 0.27 nm) of the standing-up layer indicates that the hexatriacontane molecules in the layer tilted 40.2° with respect to the surface norm, which had been observed in our previous study.[21] In addition to the parallel layers, there is a "bump" on the satellite disk, which is highlighted by the arrow in Figure 2a. The bump is about 50−60 Å higher than the parallel layer. The surface of the bump has the same phase signal as the parallel layer, suggesting that it is also covered with a layer of alkane molecules with the backbone exposed to the surface. After the spreading, the parallel layer(s) and the bump can be observed on every disk of the 30 disks that we have characterized. The exact structure of the bump still needs further investigation. On most of the satellite OTSpd disks, a patch of standing-up alkane layer also exists. We observed different heights of these standing-up patches on different disks. The measured heights of these patches are consistent with our previously reported data, which have typical height values of 5.1, 4.4, 3.9, and 3.4 nm.[21] The heights of the patches reveal that alkane molecules in these patches stand up vertically or tilt at specific angles.[21] Because the satellite disks do not connect to the main disk and liquid alkane cannot spread to the satellite disk, all alkane molecules in the satellite disk are transported through the vapor phase. Because the standing-up alkane patch is on top of the parallel layer, we can also conclude that during the vapor-transport process alkane molecules first adsorbed on the clean OTSpd surface to form parallel layers. Additional alkane formed the seaweed-shaped patches only after a few layers of parallel alkane had formed. In summary, the AFM data show that both the parallel alkane layers and the standing-up alkane layer on the satellite OTSpd disk were formed from vapor-phase transport from the main disk.

Parallel Alkane Layer on the Main OTSpd Disk Is Also from the Gas-Phase Transport. Because the alkane molecules in the vapor phase can migrate to satellite OTSpd disks through vapor-phase transport and form the parallel alkane layers, it is possible that vapor-phase alkane molecules also adsorbed on the clean OTSpd surface of the main disk and formed parallel layers before the liquid alkane spread to the surface.

Our experiment confirmed this hypothesis. We performed a spreading experiment of hexatriacontane according to Scheme 1 at 70 °C, which is 5 °C below the melting point of hexatriacontane.

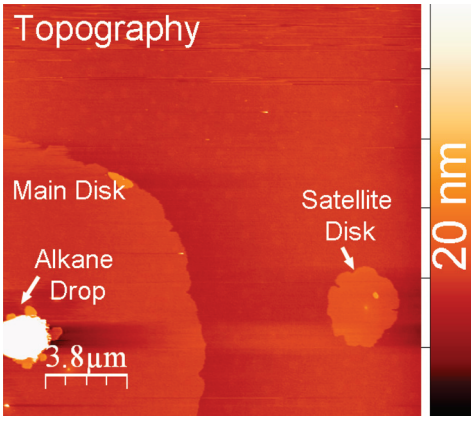

Figure 3. Hexatriacontane covered both the OTSpd main disk and the satellite disks after the sample was heated to 5 °C below the melting point of hexatriacontane. (ac mode topography image, 19 × 19 μm^2).

After remaining at 70 °C for 40 s, we cooled the sample to room temperature and characterized the pattern. Figure 3 shows the result. The alkane drop remained intact and no liquid spreading occurred, whereas the OTSpd surfaces of the main disk and the satellite disk were covered with parallel alkane layers, which appeared to be higher than OTS in the topography image. Therefore, the parallel alkane layers formed without the presence of liquid alkane. The parallel layers on the main disk also formed from the vapor-phase transport.

Our data show that the parallel layer in the alkane bilayer structure is formed from vapor-phase mass transport. Our study was conducted using discrete OTSpd patterns on the surface, but the conclusion can be extended to alkane spreading over unconstricted surfaces as well. The satellite OTSpd disks were 2−20 μm away from the main disk. In our experiments, all satellite disks were covered with parallel layers. We did not observe that the distance between the drop and the satellite disk had any impact on the formation of parallel layers. Therefore, within a 20 μm radius of the liquid hexatriacontane drop the vapor pressure of hexatriacontane is high enough to form parallel layers. On the basis of the same rationale, when an alkane drop spreads over an unconstricted, more strongly binding surface (such as on the clean SiO_2 surface of a silicon wafer), the vapor pressure of the alkane within a few micrometers of the liquid frontier would also be high enough to form a parallel alkane layer on the clean surface. As a result, when a liquid alkane drop spreads, the parallel alkane layer formed from its own vapor has already covered its peripheral area.

Conclusions

We used chemical patterns to study liquid alkane spreading. Our data showed that the parallel alkane layer on the more strongly binding surface was formed by vapor-phase adsorption, which preceded the spreading of the liquid alkane.

Acknowledgment. This research is supported by a University of Kentucky faculty start-up grant.